MULTI-CROSS-CORRELATION METHOD IN PARTICLE IMAGE VELOCIMETRY

T.-W. Hsu [*]

Department of Hydraulic and Ocean Engineering
National Cheng Kung University
Tainan, Taiwan 70101, R.O.C.

C.-Y. Shin [**]

Institute of Ocean Technology and Marine Affairs
National Cheng Kung University
Tainan, Taiwan 70101, R.O.C.

S.-H. Ou [***]

Department of Environmental Resources Management
Tajen University
Pingtung, Taiwan 90741, R.O.C.

Y.-T. Li [**]

Institute of Ocean Technology and Marine Affairs
National Cheng Kung University
Tainan, Taiwan 70101, R.O.C.

ABSTRACT

A multi-cross-correlation method (MCCM) was developed in a particle image velocimetry (PIV) auto-processing system to reduce spurious vectors and improve accuracy of measurements. This technique is an improvement based on conventional cross-correlation method (CCM). Four typical neighboring interrogation windows were specified to be overlapped and calculated by MCCM. A high cross-correlation value is obtained in which many particle images match up with their corresponding spatially shifted partners, and small cross-correlation peaks due to interference of noises during experiments are reduced. Several parameters such as out-of-plane motions, particle size, and seeding density are considered for checking both MCCM and conventional PIV algorithms. The examination gives authenticity to the merits of MCCM for avoiding particles loss or mistaken velocity vectors.

Keywords : MCCM, PIV, Cross-correlation interrogation method.

1. INTRODUCTION

Flow velocity measuring techniques have been playing a key role in understanding the fluid mechanics in many applications. Particle image velocimetry (PIV) has been widely used in many fluid researches due to its adoption of the average velocity in the interrogation areas using correlation functions. It is even applicable to measuring areas close to unsteady boundaries requiring only medium particle image density. Nowadays, the achievements in optics, lasers, electronics, videos and computer techniques have greatly promoted the employment of PIV in much more fluid flow studies with increasing spatial and temporal accuracies once exclusively possessed by laser Doppler velocimetry (LDV) (Raffel *et al*. [1]; Grue *et al*. [2]). Recently, the function of PIV has been rapidly extended to measure multiphase flows using image processing techniques (*e.g.* Chang and Liu, [3]; Chang *et al*. [4]). We can expect that PIV and image measurement method will play an important role in the future development of modern hydrodynamics.

For PIV image processing, there are four major procedures including: (1) image acquisition; (2) velocity vector field calculation using auto- or cross-correlations; (3) sub-pixel fix estimates and (4) data validation and false vector correction. Several well-validated analytical techniques are generally introduced in the PIV processing. Detailed studies can be found in many previous publications, such as Keane and Adrian [5]; Raffel and Kompenhans [6]; Dracos [7]; Raffel *et al*. [1]; Shavit *et al.* [8] and others. For the first process, to reduce and eliminate false vectors, noise signals should be first carefully avoided in the processes of image recording embracing illumination, seeding and recording devices. Secondly, noise signals have to be removed during the image processing when calculating brightness, relative coordinates and particle images. For the velocity vector generation, the cross-correlation statistics was implemented to improve calculation accuracy (Keane and Adrain, [9]). For the third procedure, to avoid bias errors by achieving sub-pixel accuracy, the three-point Gaussian curve-fitting method was also frequently adopted in the image processing algorithms (Willert and Gharib, [10]; Huang *et al*. [11]). For the last step, output from two-dimensional (2D) PIV systems that are based on optical or numerical cor-

[*] Professor, corresponding author [**] Graduate student [***] Professor

DOI : 10.1017/jmech.2011.39
Copyright © 2011 The Society of Theoretical and Applied Mechanics, R.O.C.
https://doi.org/10.1017/jmech.2011.39 Published online by Cambridge University Press

relation methods consists of an equally 2D space grid of vectors. These vectors may be false measurements or spurious vectors due to the unmatched particle pairs. In this case, the accuracy and reliability of measurements become uncertain. Therefore, some data validations such as detection, removal and replacement of spurious vectors by correct ones have been addressed by many researchers (*e.g.* Westerweel [12]; Huang *et al*. [13]; Huang *et al*. [14]; Veber *et al*. [15]). Methods for removal of erroneous vectors have been proposed by Huang *et al*. [14]; Westerweel [12]; Yamamoto *et al*. [16]; Nogueira *et al*. [17]; Falchi *et al*. [18]; Shavit *et al*. [8]; Brevis *et al*. [19] and others.

The methods to detect false vectors are developed based on fluid flow. If the calculated vectors by correlation method are incorrect, the refinement still remains uncertainty to some extent. This is due to the fact that average vectors are routinely used for replacing uncertain vectors by an interpolating method from surrounding vectors which may not be high quality results. An alternative was proposed by Nogueira *et al*. [17] using a interpolating algorithm of filter which is referred to as a scalar amplification of each velocity component a_{ij} and of a filter output $b_{0,0}$, in which the filter is defined by $b_{0,0} = \sum a_{ij}\,\eta_{ij} / \alpha$, where η_{ij} is the measuring velocity vector, $\alpha = \sum a_{ij}$ and the filter impulse response is a_{ij} / α. A higher value of amplification could be produced as a close comparison with neighboring points is obtained. However, with this class of filters, null amplification cannot be avoided for a combination of frequencies. This implies that it is not easy to achieve a higher accurate PIV processing using the interpolating filter.

In PIV, two sequential digital images are subsampled at one particular area by an interrogation window as shown in Fig. 1. The average velocity of particles within these interrogation windows can be calculated by $V = \Delta S / \Delta t$, where ΔS is the average spatial shift and Δt is the time interval between two sequential images. The discrete cross-correlation function $R(m, n)$ of the sampled interrogation windows X and Y is given by $R(m, n) = \sum_i \sum_j [X(i, j)Y(i-m, j-n)] \Big/ \sqrt{\sum_i \sum_j X^2(i, j)} \sqrt{\sum_i \sum_j Y^2(i-m, j-n)}$, where $X(i, j)$ and $Y(i, j)$ are the particle image pairs in the first and second exposed images, respectively, and (i, j) and (m, n) are the indices and the displacements of the interrogation template, respectively. The location of the correlation peak is directly associated with the particle displacement in the PIV techniques. The most three commonly used fitting methodologies for PIV processing are center of mass, parabolic fit and Gaussian curve-fitting method (GCFM) (Grue *et al*., [2]), in which GCFM is generally recognized as a popular technique for academic community and commercial software to obtain the correlation peak within a sub-pixel accuracy.

According to Huang *et al*. [11], it is assumed that the correlation peak has a Gaussian-distribution shape and

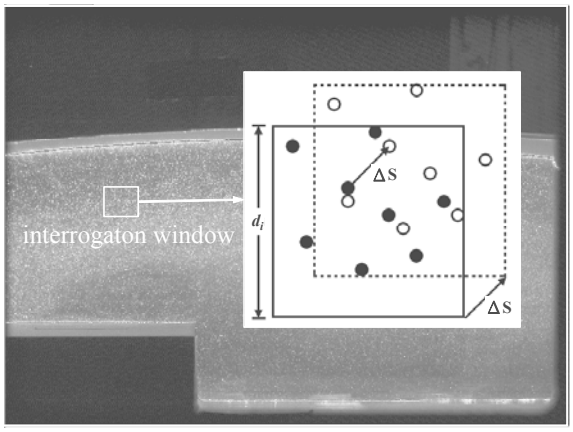


Fig. 1 An interrogation of sub-sampling images associated with PIV

the accurate location of the correlation peak can be estimated by GCFM. Note that a maximum cross-correlation value indicates an average movement of the particles in an interrogation window for GCFM. If there exists the other cross-correlation value larger than the maximum value in a complicated flow field, the average movement may be wrong and could produce an erroneous vector. This indicates that GCFM is limited for the case of several uncertain noises, such as out-of plane motion (in strong 3D flow), the number of the particle size, velocity gradients, and the number of particles *etc*. Because these factors would disturb the estimation of the maximum cross-correlation value and result in a false velocity vector.

To obtain a more correct estimation of cross-correlation, Shavit *et al*. [8] provided an image-enhancement procedure for improving PIV results when bright spots are present in the images. It can be applied when using either commercial or open-source PIV codes. Being a simple modification to the images, intensity capping is computationally cheap and easy to implement. A new robust evaluation of the dissimilarity between interrogation windows in image velocimetry is proposed by Falchi *et al*. [18] and its effectiveness in velocity evaluation is compared versus a cross-correlation based algorithm. An integrated cross-correlation/relaxation algorithm for particle tracking velocimetry is presented by Brevis *et al*. [19]. The method is based on the improvement of the individual performance of both matching methods by combining their characteristics in a two-stage process. The results show that in case of high velocity gradients and heterogeneous seeding, the integrated algorithm improves the overall performance of the individual algorithms.

Hart [20] proposed a non-post-interrogation method to reduce subpixel errors and eliminate spurious vectors from PIV results. This method is based on an element-by-element comparison of the correlation tables taken from neighboring regions. Many overlapped sub-windows were subdivided and calculated the correlation values. The overall spatial shift is in terms of a peak by co-calculating and integrating the new correlation relation from adjacent regions. The full field is split many overlapping small windows which may make

https://doi.org/10.1017/jmech.2011.39 Published online by Cambridge University Press

the processing and calculation too complicated and laborious.

For reducing spurious vectors and increasing accuracy and reliability of measurements for flow field, a new PIV calculation method to estimate the accurate location of the correlation peak is proposed in this paper. The multi-cross-correlation method (MCCM) is inspired from Hart [20] and is implemented in the auto-processing system to enhance the accuracy of data analysis from measured vector fields. We present many typical examples and an experiment for waves propagating over a submerged breakwater to examine the validity of MCCM. The results showed that MCCM processing with four sub-windows is highly effective for resolving particle displacements to reduce spurious vectors by PIV. The new result improves particle images matched up by their corresponding spatially shifted partners and interference of noises during experiments.

2. HIGHER ORDER ACCURACY OF PIV ALGORITHM

2.1 Gaussian Curve-Fitting Method (GCFM)

A comparison of velocity errors of numerical simulations between PIV cross-correlation computation with and without GCFM for linear translation is demonstrated in Fig. 2. For a brief comparison, the adopted absolute errors Er_u and Er_v in planar Cartesian coordinates of x and y directions are defined, respectively, as

$$Er_u = \sum_{i=1} |ua_i - uc_i| \text{ and } Er_v = \sum_{i=1} |va_i - vc_i| \qquad (1)$$

where (ua_i, va_i) and (uc_i, vc_i) are analytical and computed velocities in both x and y directions, respectively. Figure 2 clearly illustrates that the errors are reduced to the order of 0.1 pixels by GCFM. On the other hand, we notice that the errors are generally larger with a maximum value of about 0.5 pixels without the help of GCFM. From this comparison, we thus conclude that the sub-pixel accuracy can be achieved by introducing GCFM in the PIV processing system.

2.2. Multi-Cross-Correlation Method (MCCM)

MCCM has been encountered into PIV auto-processing system to account for the correct estimation of the cross-correlation value. Following the concept of Hart [20], we use MCCM for the reduction of randomness of the cross-correlation algorithm. In this investigation, four overlapped sub-windows were co-calculated and integrated into a new correlation relation by the following formula,

$$R_0(m, n) = R_1(m, n)R_2(m, n)R_3(m, n)R_4(m, n) \qquad (2)$$

where R_0 is the new correlation value calculated by MCCM algorithm, R_1, R_2, R_3 and R_4 are the cross-correlation values of four neighboring sub-windows, respectively (see Fig. 3), and are computed by the cross-correlation algorithm as follows.

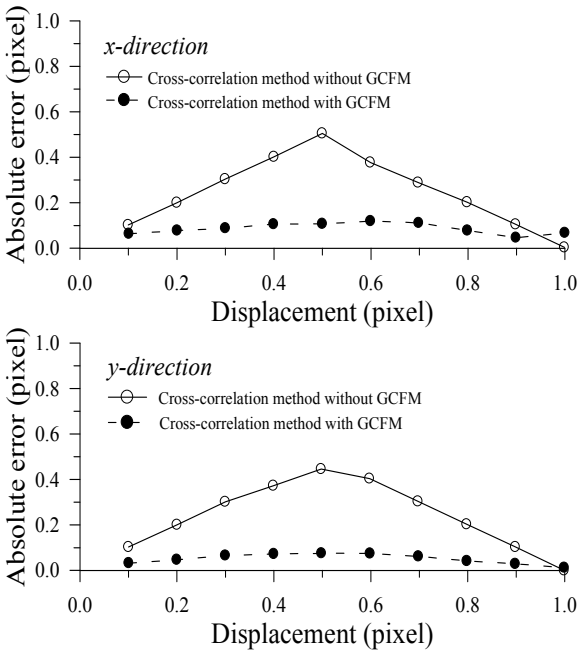


Fig. 2 A comparison of velocity errors of numerical simulations in x- and y-directions calculated by PIV cross-correlation computation with and without GCFM

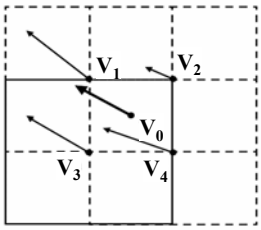


Fig. 3 Schematic sketch of MCCM

$$R_1(m, n) = \frac{\sum_i \sum_j [X_1(i, j)Y_1(i-m, j-n)]}{\sqrt{\sum_i \sum_j X_1^2(i, j)} \sqrt{\sum_i \sum_j Y_1^2(i-m, j-n)}} \qquad (3)$$

$$R_2(m, n) = \frac{\sum_i \sum_j [X_2(i, j)Y_2(i-m, j-n)]}{\sqrt{\sum_i \sum_j X_2^2(i, j)} \sqrt{\sum_i \sum_j Y_2^2(i-m, j-n)}} \qquad (4)$$

$$R_3(m, n) = \frac{\sum_i \sum_j [X_3(i, j)Y_3(i-m, j-n)]}{\sqrt{\sum_i \sum_j X_3^2(i, j)} \sqrt{\sum_i \sum_j Y_3^2(i-m, j-n)}} \qquad (5)$$

$$R_4(m, n) = \frac{\sum_i \sum_j [X_4(i, j)Y_4(i-m, j-n)]}{\sqrt{\sum_i \sum_j X_4^2(i, j)} \sqrt{\sum_i \sum_j Y_4^2(i-m, j-n)}} \qquad (6)$$

As depicted in Fig. 3, each of these sub-windows has conformable particles movement; therefore there exists a near cross-correlation peak location where the most particles move on. Figure 4 shows a typical result of PIV

https://doi.org/10.1017/jmech.2011.39 Published online by Cambridge University Press

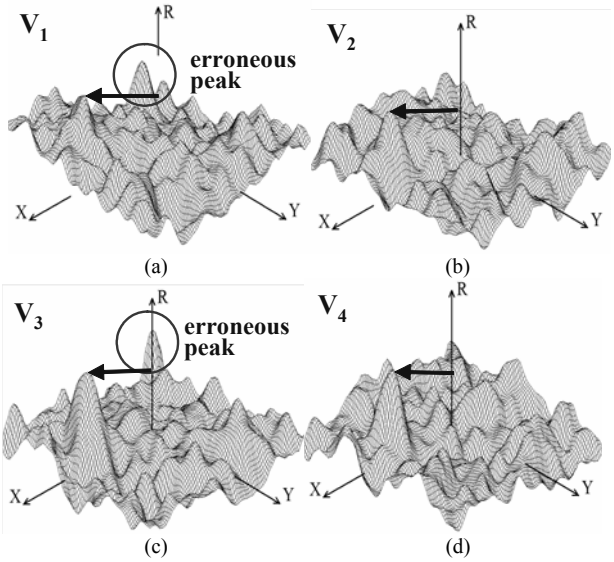


Fig. 4 Cross-correlation calculated by conventional PIV algorithm of four neighboring interrogation windows cross-correlation

cross-correlation calculation that represents extreme randomness for vector detection. Notably, uncertain noises may generate the erroneous peaks which bring about the error calculation of PIV algorithm [see Figs. 4(a) and 4(c)]. To obtain a more correct estimation of cross-correlation, these four sub-windows cross-correlation results were integrated, and the result is shown in Fig. 5. In the figure, the cross-correlation value identifies that the incorrect particle movements and values caused by randomness are notably reduced. This typical example confirms that MCCM could diminish the randomness error when cross-correlation calculation is performed.

Spurious vectors are the most commonly existing problem to PIV algorithm. They could not be avoided and may lead to inaccurate velocity results in the velocity field analysis. In conventional PIV algorithm, data validation is often used to defuse the false vectors, but the results mainly depend on data quality control. Normally, a velocity data set of better quality could produce a more accurate velocity vector field in PIV processing. However, it is difficult to accomplish a very completely qualitative data during experiments. Randomness and uncertainty noises still occur for many cases of complicated flow field. The present MCCM has the advantage to avoid data quality control problem by decreasing most of false vectors using overlapped sub-windows and consequently to increase the correct velocity vectors. To achieve this goal, typical examples are demonstrated to examine applicability of MCCM in the next section.

Figure 6 depicts *x*- and *y*-directional profiles of cross-correlation results calculated from the conventional PIV technique and MCCM. In the figure, the dash line denotes the peak of the Gaussian fitting curve using MCCM algorithm. The result of MCCM separated from Fig. 4 is also plotted for comparison. Figures 6(a) ~ 6(d) corresponding to Figs. 4(a) ~ 4(d) are shown for comparison. It is clear to see that the profile calculated

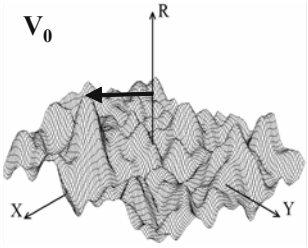


Fig. 5 Cross-correlation calculated by MCCM obtained from Figs. 4(a) to 4(d)

by MCCM is closer to Gaussian fitting curve than conventional cross-correlation method. This result means that MCCM algorithm provides a better accuracy than the conventional PIV method after GCFM processing. So far, we have found that MCCM can reduce spurious vectors and thus improve accuracy of measurements. A detailed discussion is given for this point in the following sections.

3. ACCURACY ASSESSMENTS

In this section, the validity of MCCM method is first examined by the Monte Carlo simulation. Sample images of 512 × 512 pixels were generated by the Monte Carlo simulation that has a Gaussian intensity profile with randomly located and uniformly distributed particles. This simulation has been used by many researchers such as Keane and Adrian [9]; Westerweel [21]; Keane *et al*. [22]; Cowen and Monismith [23]; Hart [20] and others. The PIV errors come from several parameters such as setting/choice of time interval, interrogation window, sheet thickness/depth field, CCD pixel/film resolution, out-of-plane motions, seeding densities, particle sizes and velocity gradients. Errors associated with high speed motion or significant 3D flow field having higher velocity in the z component exist for out-of-plane particle displacement. The poor setting might result in the false velocity vectors or particles convected out of interrogation region. A smaller interrogation window would produce particle displacements from regions with significant out-of-plane flow. A restricted sheet thickness could cause particle image to vanish within the window. The effect of these three factors is all involved in the parameter of out-of-plane motion. Therefore, three parameters of out-of-plane motions, seeding densities and particle size and velocity gradient were used to validate both MCCM and conventional PIV algorithms.

The mean-bias error and the root-mean-square (RMS) error are used as error index of the calculation. Suppose that the actual particle displacement is d_a and a number of computed N displacements d_i have been acquired, the mean-bias error d_m and RMS σ are, respectively, given by

$$d_m = \frac{\sum_{i=1}^{N}(d_i - d_a)}{N} \tag{7}$$

https://doi.org/10.1017/jmech.2011.39 Published online by Cambridge University Press

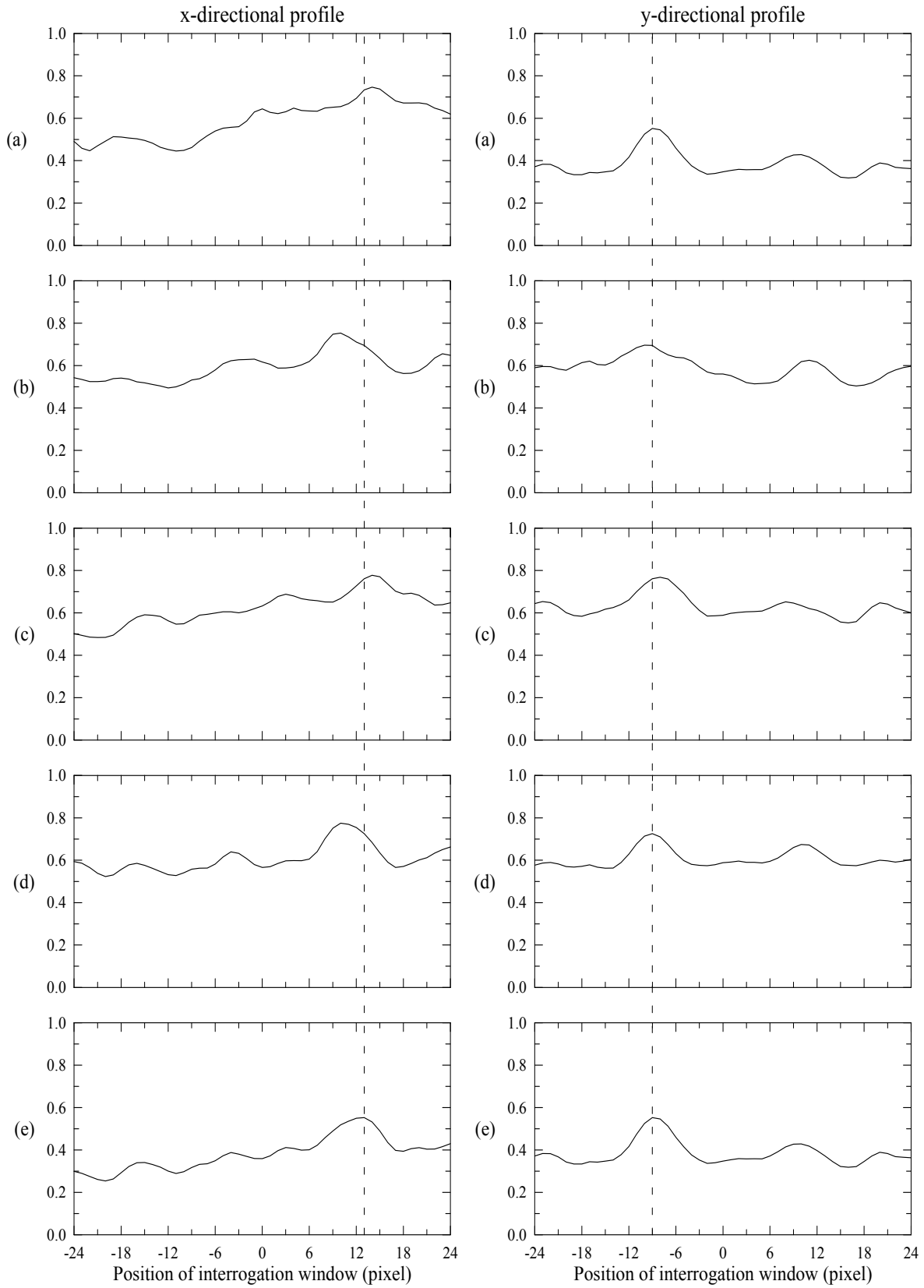


Fig. 6 *x*- and *y*-directional profiles of cross-correlation results. (a) ~ (d) calculated from conventional PIV algorithm and (e) MCCM. Dash line denotes the peak of the Gaussian fitting curve using MCCM algorithm

https://doi.org/10.1017/jmech.2011.39 Published online by Cambridge University Press

$$\sigma = \left[\frac{\sum_{i=1}^{N} (d_i - d_a)^2}{N} \right]^{1/2} \tag{8}$$

where d_m is the mean-bias error which does not fit the curve in the mean value. Simulating tests have been conducted to study these errors calculated by conventional PIV and MCCM methods.

To investigate the effect of out-of-plane motions on erroneous vectors, we generated sample images by the Monte Carlo simulation with an average seeding density of 12 particles per 32 × 32 sub-window and particle diameter of 2.4 pixels. The out-of-plane fraction 0% represents all particles in the first image remaining in the second image while 100% corresponds to no original particle remaining in the second image.

Figures 7 and 8 show the mean-bias and RMS errors for the case of the out-of-plane fraction. It is noted that the conventional PIV method can only sustain about 20% of out-of-plane motion, but MCCM reaches to 55%. This result indicates that conventional PIV algorithm could produce a great amount of spurious vectors that may occur if more than 20% of particles in the first image disappear in the second image. However, there are few false vectors existing and up to 55% of particles get lost in the second image by MCCM algorithm. For a more clear comparison, we enlarge the results of mean-bias and RMS errors as shown in Fig. 9. Obviously, the errors increase suddenly for a 20% out-of-plane motion using conventional PIV method but 55% by MCCM algorithm. Figure 10 shows the comparison of velocity vector fields for the case of the particle displacement of 0.5 pixels calculated by conventional PIV and MCCM methods. It should be noted that in the case of 60% out-of-plane motion, few correct results can be obtained by the conventional PIV method but there is a good production computed by MCCM. There are uncertain vectors appeared at 10% out-of-plane motion by the conventional PIV calculation and 60% by MCCM. It is plain that MCCM algorithm can powerfully reduce the generation of false vectors if a large number of particles get lost in the measuring area, *i.e.*, if the experiment is a strong three-dimensional flow, there are many particles might lose in the second picture and cause a incorrect algorithm by the conventional PIV method but produce a better correction by MCCM.

Figures 11 and 12 illustrate the mean-bias and RMS errors for the case of the particle displacements with 15% and 30% out-of-plane motions calculated by both conventional PIV and MCCM algorithms. A better accuracy is obtained by MCCM algorithm than conventional PIV method. This is because the correlation peak calculated by MCCM has an approximate Gaussian-distribution shape when compared with conventional PIV method. This validation supports the robustness of MCCM in removing spurious vectors and correlation anomalies.

For the second condition, seeding density is selected to verify the limitation of conventional PIV and MCCM

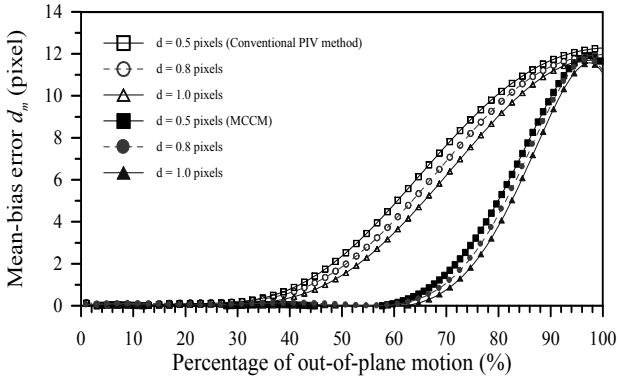


Fig. 7 Mean-bias errors for out-of-plane motions calculated by conventional PIV and MCCM algorithms

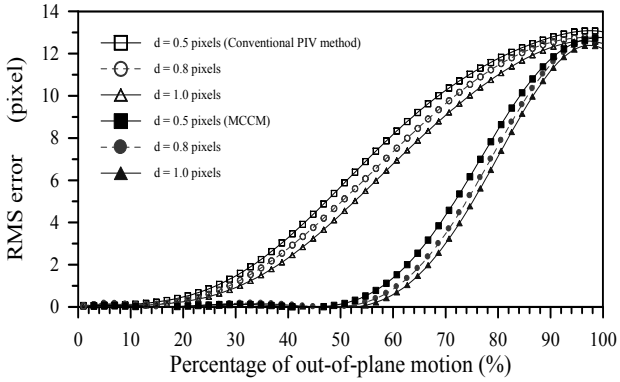


Fig. 8 RMS errors for out-of-plane motions calculated by conventional PIV and MCCM algorithms

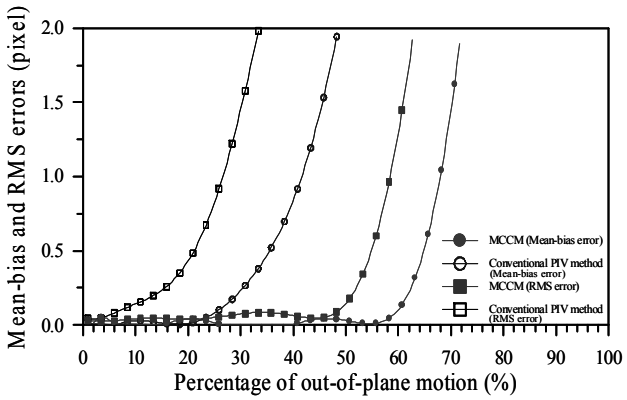
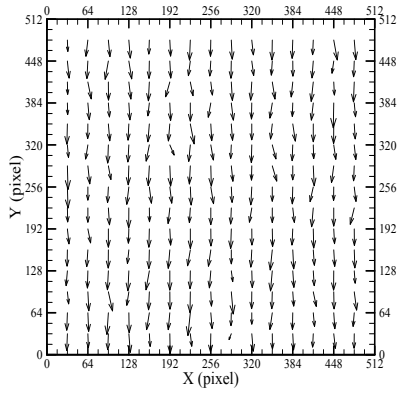


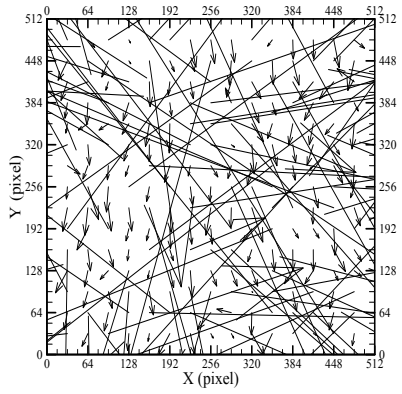
Fig. 9 The closeup of mean-bias and RMS errors as the particle displacement of 0.5 pixels for out-of-plane motions

algorithms. For convenience, we still assume the particle diameter of 2.4 pixels and without out-of-plane motion. The particle seeding density which is defined as the mean number of particles per 32 × 32 sub-window is varied from 1 to 60 particles. Figures 13 and 14 show that both values of mean-bias and RMS errors increase greatly for conventional PIV algorithm if the particle number is less than 3 particles. On the contrary, the values of mean-bias and RMS errors increase not that much for MCCM algorithm. Figure 15 shows the velocity vector fields calculated by conventional PIV and MCCM algorithms. It is apparent that a lot of spurious vectors occur at low particle density

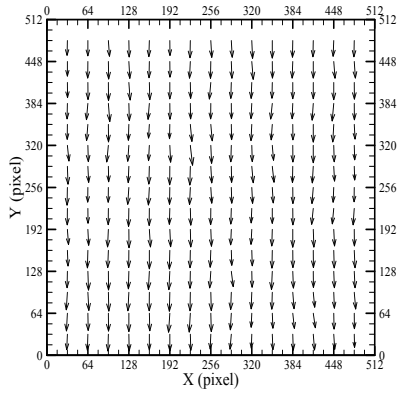
https://doi.org/10.1017/jmech.2011.39 Published online by Cambridge University Press



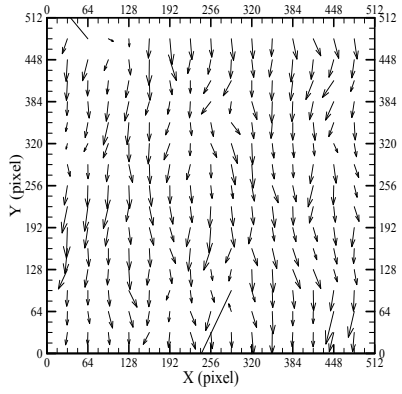
(a) 10% out-of-plane motion (conventional PIV)



(b) 60% out-of-plane motion (conventional PIV)



(c) 10% out-of-plane motion (MCCM)



(d) 60% out-of-plane motion (MCCM)

Fig. 10 Velocity vector fields (0.5 pixels displacement below) calculated by the conventional PIV and MCCM algorithms.

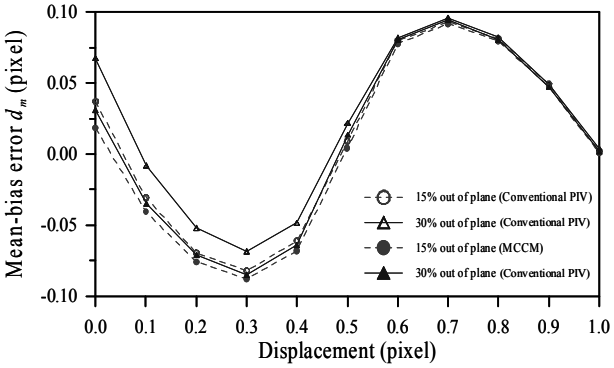


Fig. 11 Mean-bias for the case of particle displacement with 15% and 30% out-of-plane motions calculated by conventional PIV and MCCM algorithms

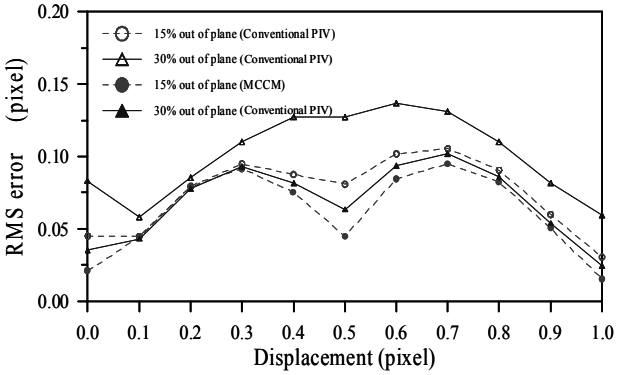


Fig. 12 RMS error for the case of particle displacement with 15% and 30% out-of-plane motions calculated by conventional PIV and MCCM algorithms

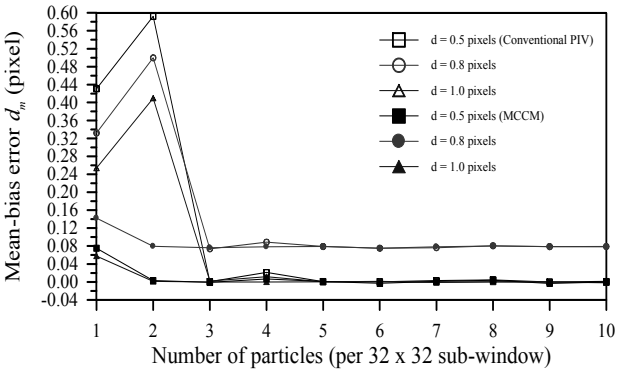


Fig. 13 Mean-bias for different particle densities

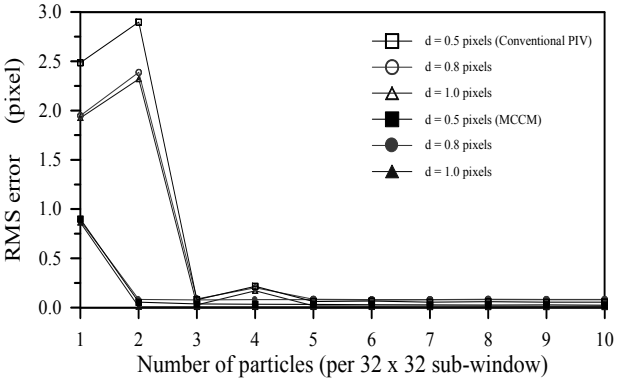
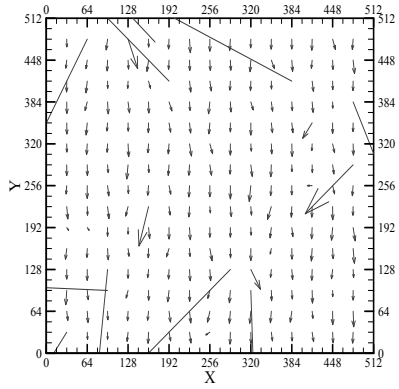
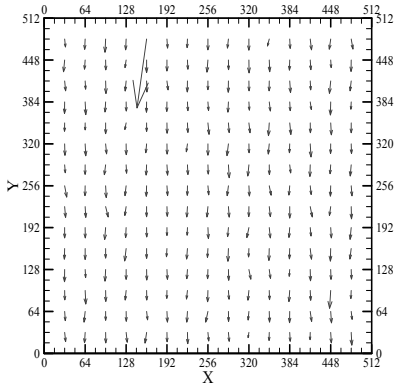


Fig. 14 RMS for different particle densities

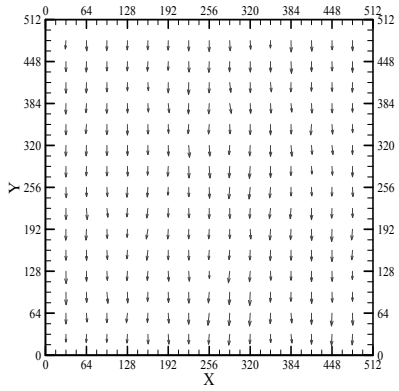
https://doi.org/10.1017/jmech.2011.39 Published online by Cambridge University Press



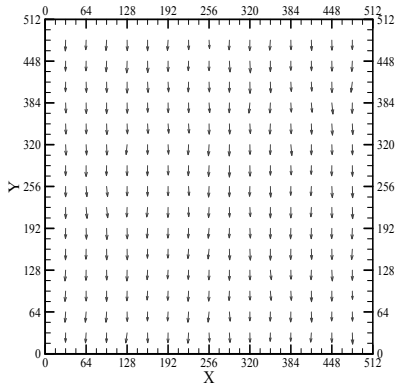
Particle number = 2 (conventional PIV)



Particle number = 4 (conventional PIV)



Particle number = 2 (MCCM)



Particle number = 4 (MCCM)

Fig. 15 Velocity vector fields (0.5 pixels displacement below) calculated by conventional PIV and MCCM algorithms with 2 and 4 particles per 32 × 32 sub-window

using conventional PIV calculation, but false vectors are decreased by MCCM calculation. This result clearly identifies that false vectors are emerged if the number of particles is too less to notice the particles movement by correlation statistics. In this condition, MCCM algorithm shows more promising results than conventional PIV algorithm. Figures 16 and 17 present the results of the application of the proposed MCCM to the data field of the particle displacements of 10 and 60 particles per 32 × 32 sub-window. The comparison shows the higher accuracy of MCCM than conventional PIV algorithm. It is concluded that reduction in seeding density could produce lots of false vectors that can be effectively reduced by MCCM.

To test the effects of particle sizes and velocity gradients on PIV processing, we choose an average seeding density of 12 particles and without out-of-plane motion, in which the particle size is varied from 0.1 pixels to 10 pixels and the gradient strength is chosen as 0, 0.03 and 0.05 pixels/pixel. The performance of conventional PIV and MCCM for the resulting mean-bias and RMS errors is depicted in Figs. 18 and 19. Since MCCM is designed to detect PIV data with overlapping of interrogation windows, the data content at wavelengths is usually small; the use of MCCM gives better results than conventional PIV algorithm. It is well known that correct flow vectors from PIV are subject to errors arisen from the tracer particle numbers, the size of the particle, velocity gradient and image resolution. Both of the particle diameter and velocity gradient play an important role to increase the resolution. Generally, the larger diameter of the tracer particle is, the more significant images are obtained so as to result in a higher autocorrelation or cross-correlation value. A small particle diameter is often biased to varying correlation degrees, because when size of particle becomes smaller it would produce noises which could reduce the estimation of the maximum cross-correlation value. When the particle diameter approaches zero, it is difficult to identify the seeding and noises, leading to errors caused by correlation anomalies. On the other hand, interesting observations by Raffel *et al*. [1] indicated that errors could increase with the increase of the velocity gradient.

In Fig. 18, it is seen that the error is smaller in the higher, but nonzero gradient case for MCCM algorithm as the particle diameter $d_p < 2$ pixel. Figure 19 shows that higher velocity gradient vectors could result in higher RMS errors from calculation of overlapped windows. It doesn't mean that the conventional PIV method is better than MCCM for particle size larger than two pixels. Notably, if we increase the velocity gradient, errors are thus produced with a small particle size (Figs. 18 and 19). The results of Figs. 18 and 19 suggest that the particle size is chosen larger than 1.6 pixels for conventional PIV and 0.7 pixels for MCCM to deliver better accurate flow field in the experiment. Figures 21 and 22 show the calculated mean-bias and RMS of a typical example in which the particle diameters of 2 and 4 pixels with a velocity gradient 0.03 pixels/pixel were selected in the simulation. It is seen that the values of MCCM are better than conventional PIV technique.

https://doi.org/10.1017/jmech.2011.39 Published online by Cambridge University Press

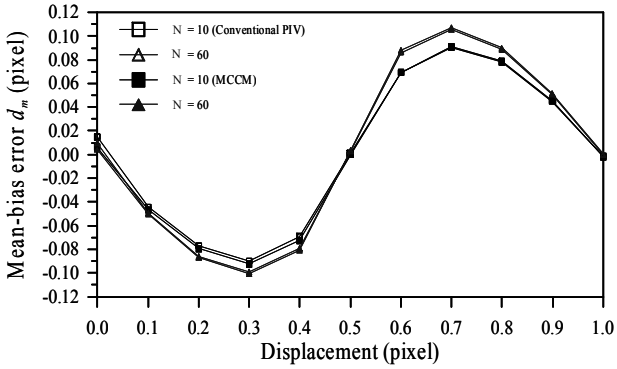


Fig. 16 Mean-bias for the particle displacement of 10 and 60 particles per 32 × 32 sub-window calculated by conventional PIV and MCCM algorithms

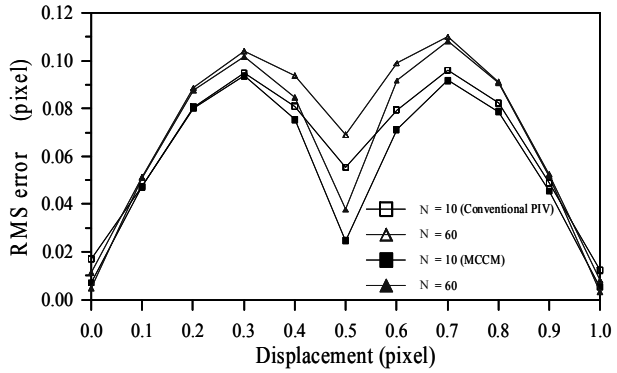


Fig. 17 RMS for the particle displacement of 10 and 60 particles per 32 × 32 sub-window calculated by conventional PIV and MCCM algorithms

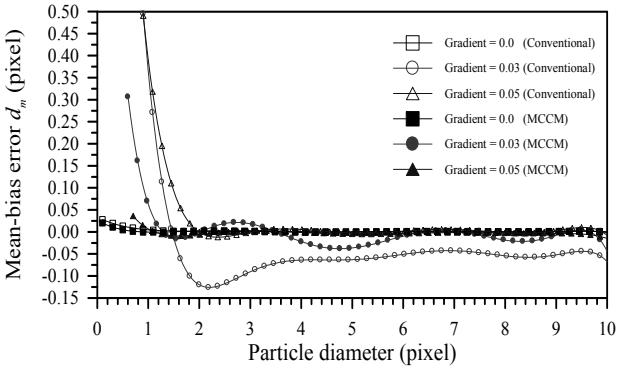


Fig. 18 Mean-bias errors for particle sizes and velocity gradients

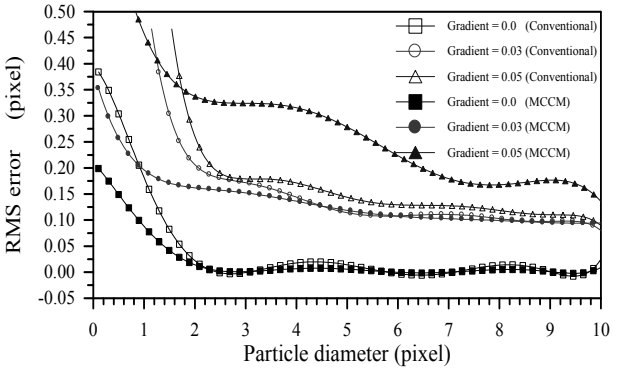
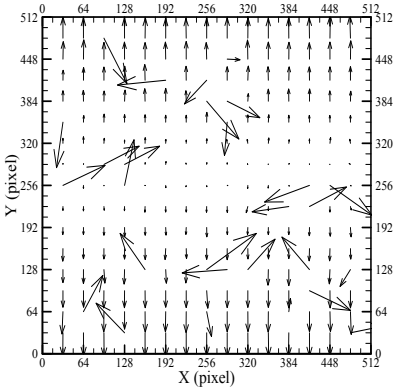
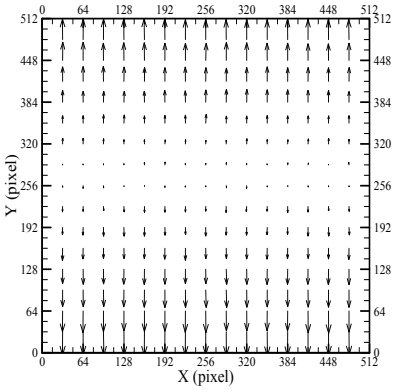


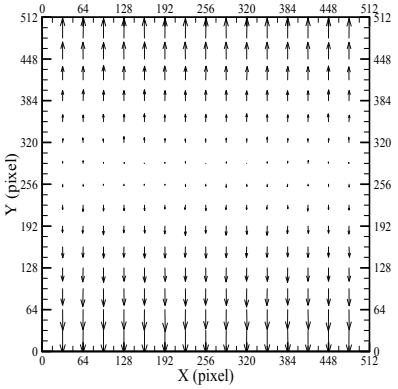
Fig. 19 RMS errors for particle sizes and velocity gradients



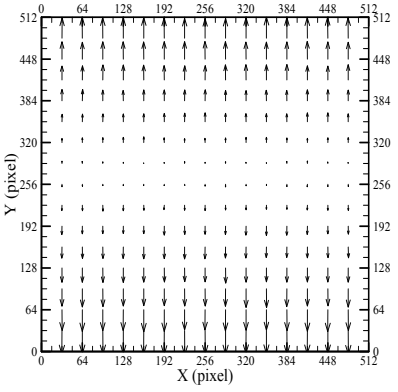
d_p = 0.8 pixels (conventional PIV)



d_p = 0.8 pixels (MCCM)



d_p = 1.8 pixels (conventional PIV)



d_p = 1.8 pixels (MCCM)

Fig. 20 Velocity vector fields calculated by conventional PIV and MCCM algorithms with a gradient velocity of 0.03 pixels/pixel and two particle sizes

https://doi.org/10.1017/jmech.2011.39 Published online by Cambridge University Press

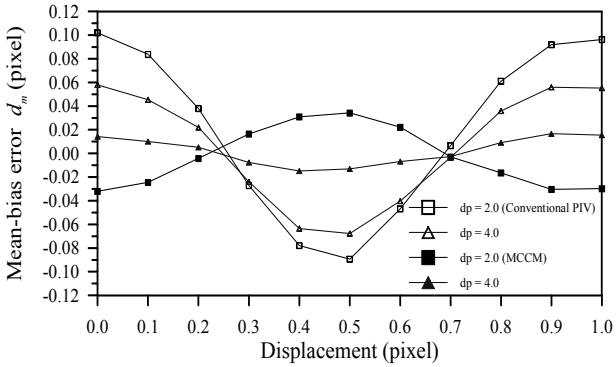


Fig. 21 Illustration of mean-bias for the particle diameters of 2 and 4 pixels with a velocity gradient 0.03 pixels/pixel calculated by conventional PIV and MCCM algorithms

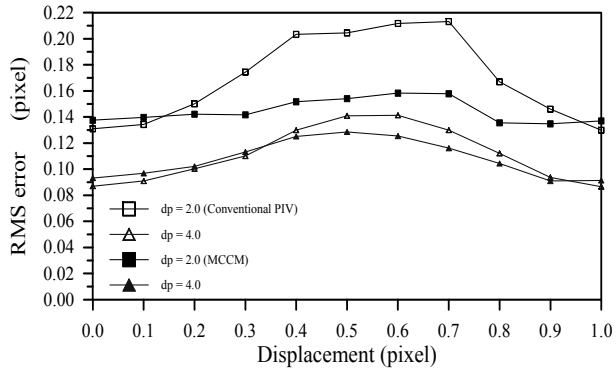


Fig. 22 Illustration of RMS for the particle diameters of 2 and 4 pixels with a velocity gradient 0.03 pixels/pixel calculated by conventional PIV and MCCM algorithms

Figure 20 provides a criterion which is helpful to define the causality of errors. In a small particle size, it is noted that conventional PIV produces several false vectors but MCCM does not. For a fixed interrogation size, MCCM processing is somewhat limited at the size of particle as aforementioned. Small particles are used in the real tests to achieve a higher accurate spatial resolution for velocity calculations. However, if the seeding particle is too small to be captured by CCD-frame camera, it cannot provide any high quality result of the velocity field. In the present investigation, we used Monte Carlo simulations to investigate the tolerance of the particle size. Results using MCCM indicate that anomalies can be eliminated when the particle diameter is smaller than 1 pixel. Therefore, it is appropriate to demonstrate the particle size effect using d_p = 0.8 pixel in Fig. 20.

4. APPLICATIONS

To verify the validity of MCCM, we performed an experiment of wave propagating over a submerged breakwater. The experiment was conducted in a wave flume of 0.5m wide, 0.6m high and 25m long. In the experiment the submerged obstacle are placed at the centred of wave flume having the dimensions of 0.5m wide, 0.1m high and 0.15m long. Regular waves were generated by an absorbing piston-type wave generator and the light source of flow visualization was radiated by a 5W Argon-ion laser beam generator (INNOVA-90, COHERENT). The flow field in the vicinity of the submerged obstacle was measured by PIV technique in the condition of the incident wave height H_0 = 4.0cm, wave period T = 2.0sec and the water depth h = 25cm.

The velocity vector field in the wave flume flow measured with a single-pulse camera pair and 45μm aluminium particles is shown in Fig. 23. The pictures illustrate the flow structures of vorticity in the vicinity of the obstacle at different phases. The velocity vectors were also computed by both conventional PIV algorithm and MCCM algorithm. As aforementioned, the existence of spurious vectors for complicated flow is mainly due to improper correlation statistics in the data processing. In this case, the velocity gradient is significant because flow pass over a corner and vortex is generated. The velocity error by using conventional PIV algorithm is mainly caused by out-of-plan if time interval is taken small enough, and the same size of the interrogation window is used to calculate the flow structure. From Fig. 23, one can observe that flow field domains are filled with velocity vectors which are unable to be generated by conventional PIV algorithm. In contrast, the central region of the flow structure is extensively dealt with by MCCM to produce a detailed flow field which closely resemble a vortex. We thus concluded that MCCM is more applicable to account for detailed complex flow than conventional PIV algorithm.

The last application of MCCM is to compute the velocity field around a submerged obstacle through comprehensive Fiber-optic Laser Doppler Velocimetry (FLDV) measurements. Several successful experiments of detecting the flow field around an obstacle induced by water waves have been performed in wave flumes. Temporal variations of flow field in a wave cycle at a fixed point for both horizontal and vertical velocity components were measured and analysed. Figure 24 presents a comparison of FLDV conventional PIV and MCCM calculation for two wave conditions: H_0 = 4.0cm, T = 1.02sec for Fig. 24(a) and H_0 = 4.0cm, T = 2.0sec for Fig. 24(b), respectively. In the figure, the dot denotes FLDV measurement, the solid line represents the results calculated by MCCM, and the dash line is the results obtained from conventional PIV method. It can be seen that the velocity vectors calculated by MCCM algorithm are in better agreement with the experimental data of FLDV than conventional PIV method.

5. CONCLUSIONS

An improved multi-cross-correlation method (MCCM) to deal with false vectors is developed in the present investigation. Further refinement for data correction and for deriving flow magnitude is proposed. The proposed MCCM is inspired from Hart [20] and

https://doi.org/10.1017/jmech.2011.39 Published online by Cambridge University Press

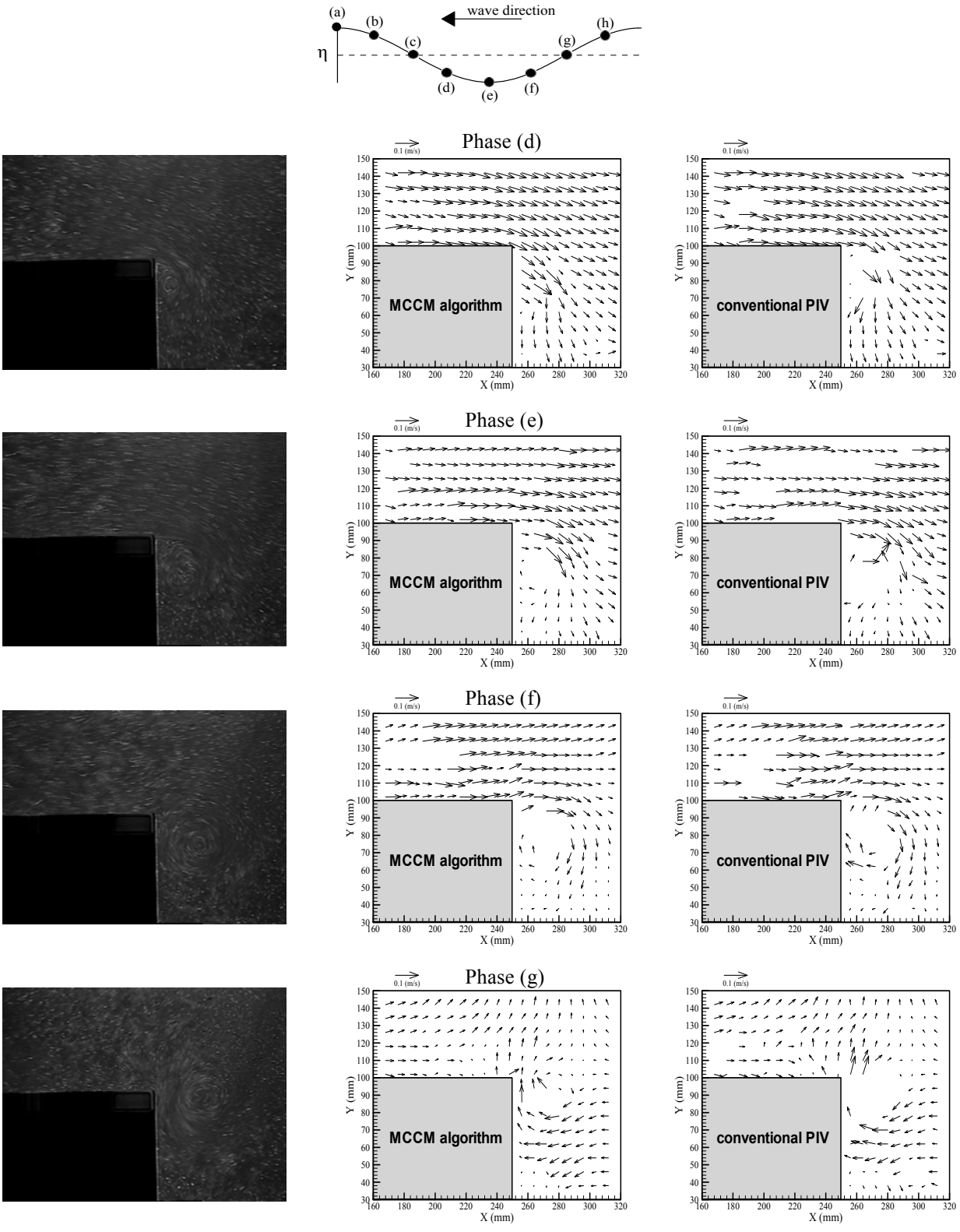


Fig. 23 Comparisons of velocity fields with two PIV processed forms and original images by flow visualization at phases (d), (e), (f) and (g)

https://doi.org/10.1017/jmech.2011.39 Published online by Cambridge University Press

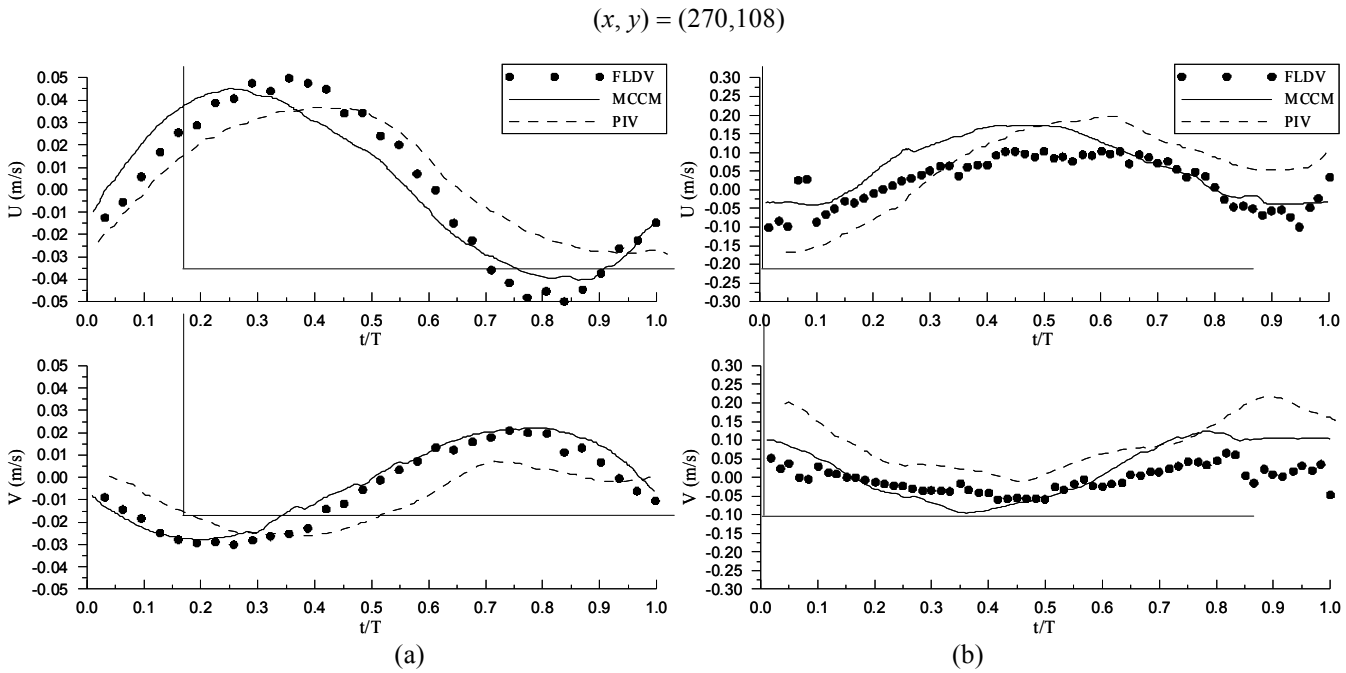


Fig. 24 Comparisons of temporal variations of both velocity components by MCCM (in solid line) PIV algorithm (in dash line) and FLDV technique (in dots) for wave periods of (a) 1.02 sec and (b) 2.0 sec.

has been shown to reduce spurious vectors detected by conventional PIV and FLDV. The present MCCM has the advantage to avoid data quality problem by reducing most of spurious vectors using four overlapping sub-windows and consequently increase the accuracy and reliability of PIV measurements for flow field.

The validity of MCCM is first examined by the Monte Carlo simulation in which three key parameters of out-of-plane motions, seeding densities, particle sizes and velocity gradients are investigated in the accuracy assessment for both MCCM and conventional PIV algorithms. It is obvious that MCCM can powerfully reduce the generation of false vectors that causes a large number of particle lost pairs in the measuring area for a strong three-dimensional flow. MCCM algorithm shows more promising results than that of conventional PIV algorithm for the case of the particle member is too less to notice the particle movement by correlation statistics.

If we increase the velocity gradient, errors are thus produced with a small particle size. The error is smaller in the higher, but nonzero gradient case for MCCM algorithm as the particle diameter is less than 2 pixel. The velocity vectors were measured by FLDV, PIV detection and calculated by conventional PIV algorithm and MCCM in a laboratory experiment. The comparison shows that correct vector fields can be reasonably produced by MCCM in the flow sub-domains where false vectors cannot be eliminated by conventional PIV.

MCCM unlike post-interrogation methods, uses all available correlation information calculated from interrogation regions and does not depend on the accuracy or similarity of neighboring vectors. Therefore, it resolves tracer particle displacement from regions that are obscured by correlation anomalies. We thus concluded that MCCM is easy to implement for reducing bias errors and eliminating false vectors in improving subpixel accuracy and vector fields.

ACKNOWLEDGEMENTS

The authors are grateful for the financial support provided by the National Science Council under grants NSC95-2811-E-127-001, NSC 96-2221-E127-006-MY3 and the Research Center of Ocean Environment, National Cheng Kung University, Tainan, Taiwan. The authors are also grateful to Dr. S.C. Hsieh, a Researcher of National Chung Hsing University, Taichung, Taiwan, for his valueable suggestions to revise the paper.

REFERENCES

1. Raffel, M, Willert, C, and Kompenhans, J, "Particle Image Velocimetry, a Practical Guide," Springer, Berlin Heidelberg New York (1998).
2. Grue, J, Liu, P, and Pedersen, G, "PIV and Water Waves," Advances in Coastal and Ocean Engineering, **9**, World Scientific, Hackensack N.J. London, 352p (2004).
3. Chang, K, and Liu, P, "Pseudo Turbulence in PIV Breaking-Wave Measurements," *Experiments in Fluids*, **29**, pp. 331–338 (2000).
4. Chang, K, Hsu, T, and Liu, P, "Vortex Generation and Evolution in Water Waves Propagating Over a Submerged Rectangular Obstacle, Part II: Cnoidal Waves," *Coastal Engineering,* **52**, pp. 257–283 (2005).
5. Keane, R, and Adrain, R, "Optimization of Particle

https://doi.org/10.1017/jmech.2011.39 Published online by Cambridge University Press

Image Velocimetry, Part I: Double Pulsed Systems," *Measurement Science and Technology,* **1**, pp. 1202–1215 (1990).
6. Raffel, M, and Kompenhans, J, "Theoretical and Experimental Aspects of Image-Shifting by Means of a Rotating Mirror System for Particle Image Velocimetry," *Measurement Science and Technology,* **6**, pp. 795–808 (1995).
7. Dracos, T, "Three-Dimensional Velocity and Vorticity Measuring and Image Analysis Techniques," Springer, Berlin Heidelberg New York (1996).
8. Shavit, U, Lowe, R. J. and Steinbuck, J. V., "Intensity Capping: A Simple Method to Improve Cross-Correlation PIV Results," *Experiments in Fluids*, **42**, pp. 225–240 (2007).
9. Keane, R, and Adrain, R, "Theory of Cross-Correlation Analysis of PIV Images," *Applied Scientific Research,* **49**, pp. 191–215 (1992).
10. Willert, C, and Gharib, M, "Digital Particle Image Velocimetry," *Experiments in Fluids*, **10**, pp. 181–193 (1991).
11. Huang, H, Dabiri, D, and Gharib, M, "On Errors of Digital Particle Image Velocimetry," *Measurement Science and Technology,* **8**, pp. 1427–1440 (1997).
12. Westerweel, J, "Efficient Detection of Spurious Vectors in Particle Image Velocimetry Data," *Experiments in Fluids*, **16**, pp. 236–247 (1994).
13. Huang, H, Fiedler, H, and Wang, J, "Limitation and Improvement of PIV, Part I: Limitation of Conventional Techniques Due to Deformation of Particle Image Patterns," *Experiments in Fluids*, **15**, pp. 168–174 (1993a).
14. Huang, H, Fiedler, H, and Wang, J, "Limitation and Improvement of PIV, Part II: Particle Image Distortion, a Novel Technique," *Experiments in Fluids*, **15**, pp. 263–273 (1993b).
15. Veber, P, Dahl, J, and Hermansson, R, "Study of the Phenomena Affecting the Accuracy of a Video-Based Particle Tracking Velocimetry Technique," *Experiments in Fluids*, **22**, pp. 482–488 (1997).
16. Yamamoto, F, Wada, A, Iguchi, M, and Ishikawa, M, "Visualization and Image Processing of Torque Converter Internal Flow," *Journal of Flow Visualization Image Proceedings,* **3**, pp. 51–64 (1996).
17. Nogueira, J, Lecunoa, A, and Rodriguez, P, "Data Validation, False Vectors Correction and Derived Magnitudes Calculation on PIV Data," *Measurement Science and Technology,* **8**, pp. 1493–1501 (1997).
18. Falchi, M, Querzoli, G, and Romano, G. P., "Robust Evaluation of the Dissimilarity Between Interrogation Windows in Image Velocimetry," *Experiments in Fluids*, **41**, pp. 279–293 (2006).
19. Brevis, W, Nino, Y, and Jirka, G. H, "Integrating Cross- Correlation and Relaxation Algorithms for Particle Tracking Velocimetry," *Experiments in Fluids*, DOI 10.1007/S00348-010-0907-Z. (2010).
20. Hart, D. P., "PIV Error Correction," *Experiments in Fluids*, **29**, pp. 13–22 (2000).
21. Westerweel, J, Digital Particle Image Velocimetry-Theory and Application, PhD Dissertation, Delft University Press, Delft, The Netherlands (1993).
22. Keane, R, Adrian, R, and Zhang, Y, "Super-Resolution Particle Image Velocimetry," *Measurement Science and Technology,* **6**, pp. 754–768 (1995).
23. Cowen, E, and Monismith, S, "A Hybrid Digital Particle Tracking Velocimetry Technique," *Experiments in Fluids*, **22**, pp. 199–211 (1997).

(Manuscript received June 8, 2010,
accepted for publication September 13, 2010.)

https://doi.org/10.1017/jmech.2011.39 Published online by Cambridge University Press